Check for updates

Covalent organic imine polymer containing benzothiadiazole as a bifunctional material for specific fluorescence detection and removal of Hg²⁺

Yunrui Gao, Hao Chen, [ID] Hanxun Zou* and Hang Chen [ID] *

As one of the most toxic heavy metals to humans and the environment, achieving simultaneous fluorescence detection and effective removal of Hg²⁺ presents a significant challenge. In this study, we combined the excellent photoelectric properties of benzothiadiazole groups with the porous structure of covalent organic polymers (COPs) to develop a novel covalent organic polymer material (**BTD-MPD-COP**) with enhanced fluorescence performance. The benzothiadiazole-modified sites in this material achieved the bifunctional application of **BTD-MPD-COP** for Hg²⁺ fluorescence detection with a detection limit of 35.65 μM and simultaneous removal with a capacity of 475 mg g⁻¹. Furthermore, **BTD-MPD-COP** demonstrated remarkable Hg²⁺ selectivity and can be reused after desorption without significant reduction in its adsorption capacity. This indicates that **BTD-MPD-COP** possesses excellent dynamic reversibility in the adsorption of Hg²⁺. In summary, the development of functionalized bifunctional covalent organic polymer materials presents an effective strategy for simultaneous removal and detection of toxic heavy metal ions.

Introduction

Heavy metal ions are a primary contributor of current environmental pollution, and these pollutants pose a serious threat to human health.[1–6] Among these pollutants, Hg²⁺ is regarded as one of the most detrimental heavy metal ion contaminants, representing a substantial risk to both human well-being and the ecological environment.[7–12] Therefore, developing a highly sensitive detection system for Hg²⁺ is of paramount importance, which can help to identify the existence of hazardous sources in a timely manner and eliminate them promptly. Currently, various strategies have been devised to mitigate pollution caused by heavy metal ions, including chemical precipitation,[13,14] solvent extraction,[15,16] membrane separation,[17,18] adsorption[19–22] and so on. However, each of these treatment techniques presents technical and economic challenges while also being complex and time-consuming in their operational processes. The adsorption method is regarded as one of the most effective ways to remove heavy metals due to its simplicity and low cost. By creating efficient adsorbents specifically designed for this purpose, it is anticipated that this approach will prove effective in eliminating Hg²⁺. Moreover, the optical

detection method based on fluorescence or colorimetric changes has become the most convenient and effective method due to their simplicity, rapid response times, and low detection limit, which has become a useful tool for Hg²⁺ detection.[23–26] Consequently, there is an urgent need for the development of new functional materials that exhibit high adsorption capacity along with excellent selectivity and stability.

Therefore, the concept of designing dual-functional materials capable of both detecting and efficiently removing Hg²⁺ has garnered significant attention. In recent years, various materials such as hydrogels,[27,28] supramolecular polymers,[29] metal–organic frameworks (MOFs),[30,31] and covalent organic frameworks (COFs)[32] have been employed for the adsorption of Hg²⁺. However, the long reaction time, complex purification process, and poor repeatability associated with these synthetic conditions have largely constrained their potential in practical dual-functional applications. Among these materials, covalent organic polymers (COPs) as a new type of functional material have attracted much attention in the field of materials science due to their unique topological configuration and customizable molecular properties.[33–36] As a type of porous material connected by robust covalent bonds (such as imine bonds), COPs exhibit great promise in catalysis,[37] adsorption,[38] energy storage,[39] and chemical sensing[33,40] due to their high specific surface area, adjustable pore size, excellent structural stability, and abundant functional sites. In comparison to COFs, the tight stacking order between layers of COFs usually leads to a strong

Fujian Provincial Key Laboratory of Ecological Impacts and Treatment Technologies for Emerging Contaminants, Key Laboratory of Ecological Environment and Information Atlas, College of Environmental and Biological Engineering, Putian University, Putian, Fujian 351100, PR China

aggregation-induced quenching (ACQ) effect, resulting in poor fluorescence detection performance.[41] The disordered structure of COPs can mitigate the ACQ effect. Furthermore, COPs feature a rich conjugated system that enhances electron transport capabilities while exhibiting strong fluorescence characteristics. Consequently, they may represent ideal dual-functional materials for both fluorescence detection and removal of Hg^{2+}.

The conventional COPs typically exhibit weak interactions with Hg^{2+}, leading to suboptimal performance in the rapid detection and removal of this ion. To develop efficient, dual-functional materials for the swift detection and elimination of Hg^{2+} in aqueous solutions, it is essential to modify COPs by incorporating functional groups that bestow them with these dual capabilities. In this study, we combined the excellent photoelectric properties of the benzothiadiazole group with the unique porous structure inherent to COPs to construct a novel covalent organic polymer known as **BTD-MPD-COP**. Owing to its rich π-conjugated network, stable porous architecture, and sulfur-functionalized groups, this material demonstrates sensitive fluorescence detection alongside effective removal of Hg^{2+} from aqueous environments.

Results and discussion

The benzothiadiazole-modified COP (**BTD-MPD-COP**) was synthesized through imine condensation of aldehydes and amines, as illustrated in Scheme 1. The process involved dissolving benzothiadiazole (**BTD**)-containing monodialdehyde and *m*-phthalimide (**MPD**) in an appropriate volume of DMF solution. After thorough mixing and ultrasonic treatment for 1 hour, the mixture was transferred to a 25 mL reaction vessel and placed in an oven at 180 °C for 72 hours. Following cooling to room temperature, the crude product underwent three washes with DMF followed by anhydrous ethanol. The final product was vacuum-dried at 90 °C for 24 hours, yielding a approximately 85% reddish-brown powder.
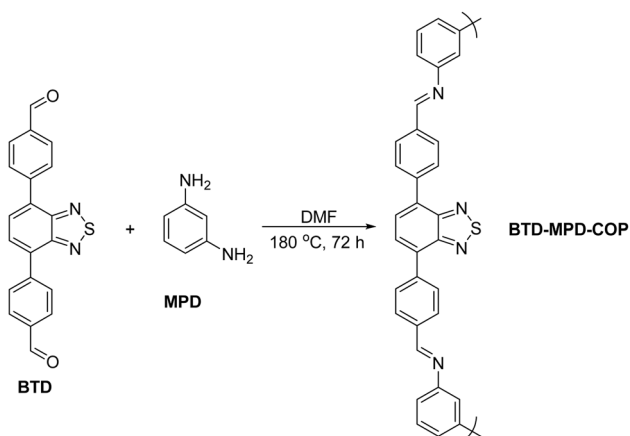
The Fourier Transform Infrared Spectroscopy (FT-IR) analysis revealed a strong N–H peak at 3000 cm^{-1} corresponding to *m*-phenylenediamine, which gradually diminished in **BTD-**

MPD-COP, indicating complete consumption of the amine component. A new C=N peak emerging at 1623 cm^{-1} confirmed the successful synthesis of imine bonds as well as thiazole-containing organic covalent materials (Fig. 1a). Furthermore, the stability of **BTD-MPD-COP** was investigated. The thermogravimetric analysis (TGA) was conducted under nitrogen atmosphere to investigate the stability of **BTD-MPD-COP** which demonstrated that **BTD-MPD-COP** exhibited no significant weight loss below 450 °C, indicating structural stability up to this temperature. At 800 °C, approximately 50% of the material remained intact, thereby demonstrating the high thermal stability of our covalent organic polymer (Fig. 1b). In order to investigate the surface structural characteristics of the material, the scanning electron microscope (SEM) was employed to observe its morphology (Fig. 1c). **BTD-MPD-COP** displayed a relatively regular spherical structure with uniformly sized pores alongside multiple pores of varying dimensions, which effectively provided channels for Hg^{2+} adsorption. Nitrogen adsorption–desorption experiments conducted at 77 K revealed isotherms consistent with Type IV N_2 adsorption profiles—a hallmark characteristic indicative of mesoporous materials.[42] The calculated specific surface area of **BTD-MPD-COP** was found to be 47.9 m^2 g^{-1} with pore diameters measuring approximately 20.5 nm, further substantiating its mesoporous properties (Fig. 1d).

And then the selective fluorescence detection properties of COP materials for heavy metal ions in aqueous solutions were investigated. Among ten common metal ions, only Hg^{2+} significantly quenched the fluorescence signal of **BTD-MPD-COP**. Fig. S1 and 2a, respectively demonstrated the fluorescence emission spectra and relative luminescence intensity changes of **BTD-MPD-COP** after metal ion addition. The quenching of the fluorescence intensity may be caused by the interaction between S atoms and Hg^{2+} in the **BTD-MPD-COP** structure, which hindered the excited proton transfer process.[43]

In order to further investigated the competitive experiment of **BTD-MPD-COP** for Hg^{2+} detection, the effects of other metal ions on fluorescence intensity changes were tested before and after adding Hg^{2+} (Fig. 2b). The results showed that when competitive metal ions were present, the emission intensity of **BTD-MPD-COP** solution significantly decreased after Hg^{2+} addition, indicating that these competing ions can not interfere with Hg^{2+} detection. These findings demonstrated that our **BTD-MPD-COP** exhibits high selectivity for Hg^{2+} detection.

To accurately assess the detection sensitivity of **BTD-MPD-COP** for Hg^{2+}, the real-time fluorescence titration experiments were conducted. As shown in Fig. 3a, the fluorescence intensity of **BTD-MPD-COP** gradually decreased to 89% through adding 1.0 mM Hg^{2+}. Based on the titration results, the quenching coefficient K_{SV} was calculated using the Stern–Volmer equation:[44] $I_0/I = 1 + K_{SV}$ (mM), where I_0 and I represent the fluorescence intensity before and after analyte addition. Fig. 3b demonstrated the excellent linear relationship between **BTD-MPD-COP** and the Stern–Volmer equation in detecting Hg^{2+}, with a K_{SV} value of 109.401 mM^{-1}. Subsequently, the detection limit (LOD) of **BTD-MPD-COP** for Hg^{2+} was determined as 35.65 μM (Fig. S2), indicating that this fluorescent probe exhibited

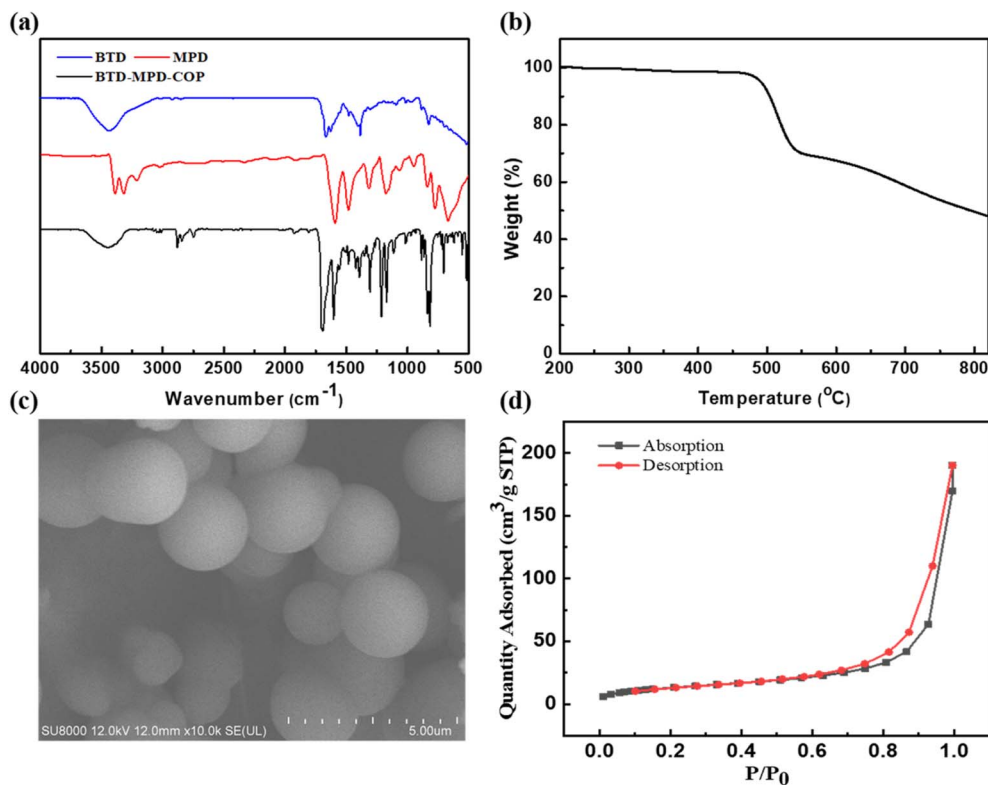
Scheme 1 Synthetic routes of BTD-MPD-COP.

Fig. 1 (a) FT-IR spectra of BTD (blue), MPD (red) and BTD-MPD-COP (black) in the wavenumber range 500–4000 cm^{-1}. (b) TGA Cures of BTD-MPD-COP under an N$_2$ atmosphere. (c) SEM images of BTD-MPD-COP. (d) N$_2$ adsorption–desorption isotherms of BTD-MPD-COP.

superior performance in Hg^{2+} detection compared to other studies (Table S1).

In addition, **BTD-MPD-COP** was left undisturbed with ten different 0.01 mol L^{-1} metal ion aqueous solutions for approximately 24 hours. EDS analysis was performed after drying the materials (Fig. S3). The postadsorption material exhibited a structure composed of multiple spherical aggregates with uneven surfaces. This phenomenon likely arises from the adsorption of mercury or other metal ions on the surface, which occupies available spaces and leads to particle aggregation.

Comparative analysis of elemental distribution patterns and layers revealed that metal elements were uniformly and randomly distributed across the material surface. As shown in Table S2, **BTD-MPD-COP** primarily adsorbed mercury ions, with the mercury content in the material reaching 75.88%, which indicates the presence of mercury adsorption on the surface of the material. Notably, the mercury content was at least ten times higher than that of other metal ions, demonstrating that **BTD-MPD-COP** exhibits superior selectivity for mercury ions.
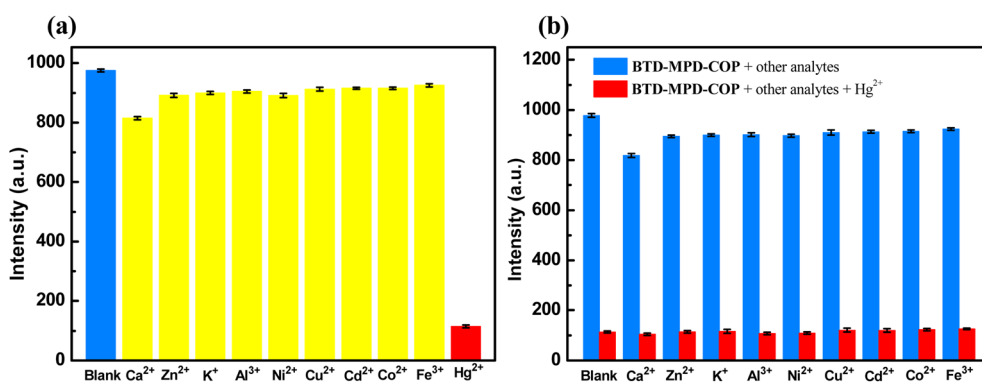

Fig. 2 The luminescence intensities of the COPs after adding different metal ions in DMSO solution (1 × 10^{-3} M). (a) **BTD-MPD-COP**; (b) the luminescence intensities of **BTD-MPD-COP** after adding other metal ions (10^{-3} M) except Hg^{2+} (black bars) and upon adding Hg^{2+} (10^{-3} M) to the above solutions (red bars);
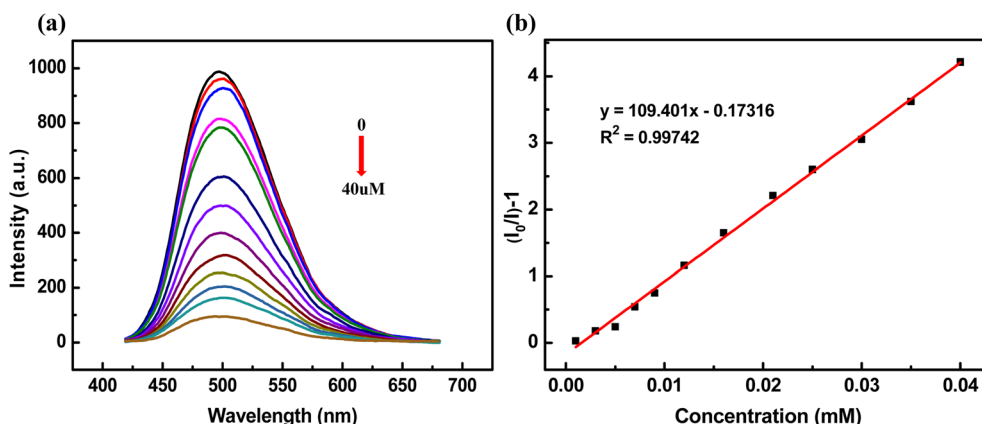
Fig. 3 (a) The fluorescence titration of **BTD-MPD-COP** dispersed in DMSO solution after gradually adding Hg^{2+}; (b) Stern–Volmer plots of **BTD-MPD-COP** for Hg^{2+}.

As a bifunctional material, **BTD-MPD-COP** not only demonstrated excellent fluorescence detection performance but also exhibited a high adsorption capacity for Hg^{2+}. Therefore, the absorption and removal characteristics regarding Hg^{2+} in aqueous solution were further investigated. Fig. 4a illustrates the adsorption kinetics model of **BTD-MPD-COP**, the experimental results indicated that in an initial Hg^{2+} concentration of 600 mg L^{-1}, the equilibrium adsorption capacity reached approximately 475 mg g^{-1} within about one hour of reaction

time and approximately 80% of this capacity was achieved during this period. This is primarily attributed to the uniform pore size and large specific surface area of **BTD-MPD-COP** material, which creates strong adsorption forces between the material sites and mercury ions. These characteristics correspond to the specific surface area results obtained from BET tests.

Circulation performance is another critical aspect in practical applications. We found that **BTD-MPD-COP** materials pre-
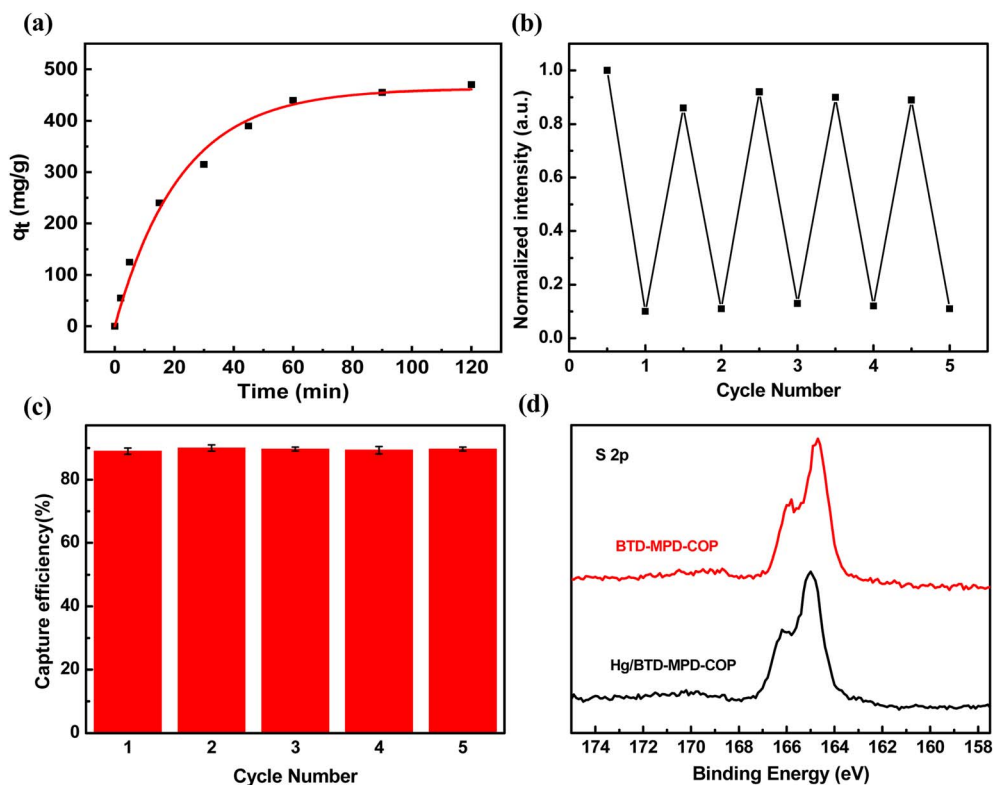

Fig. 4 (a) Adsorption kinetic model of **BTD-MPD-COP**. (b) Recycle use of **BTD-MPD-COP** for fluorescence detection of Hg^{2+}. Upon treatment in aqueous H_2SO_4–NaCl solution. (c) Recycle performance of **BTD-MPD-COP** for facile removal of Hg^{2+} in aqueous solution. Upon treatment in aqueous H_2SO_4–NaCl solution. (d) The XPS spectra of S 2p.

adsorbed with Hg^{2+} can be effectively desorbed using an H_2SO_4–NaCl solution, and the treated material was easily regenerable. The regenerated **BTD-MPD-COP** can be reused for subsequent Hg^{2+} detection and removal processes. Notably, the fluorescence property of the regenerated **BTD-MPD-COP** was also recovered completely (Fig. 4b). After the adsorption–desorption cycle of Hg^{2+} was repeated five times, the sensitivity and responsiveness of **BTD-MPD-COP** remain virtually unchanged, and the Hg^{2+} uptake of **BTD-MPD-COP** almost retained 90% of the original Hg^{2+} capacity (Fig. 4c). These results indicate that **BTD-MPD-COP** material is chemically stable in the desorption process and has excellent recycling performance.

In order to further confirm the S–Hg interaction in **BTD-MPD-COP** for selective detection and effective removal of Hg^{2+}, X-ray photoelectron spectroscopy (XPS) was employed to analyze the changes before and after **BTD-MPD-COP** adsorbed Hg^{2+}. The binding energies (BE) of S 2p in **BTD-MPD-COP** and Hg/**BTD-MPD-COP** were measured at 164.73 eV and 165.02 eV, respectively (Fig. 4d). Compared with **BTD-MPD-COP**, Hg/**BTD-MPD-COP** exhibited a positive shift of 0.29 eV for the S binding energy, confirming the interaction between Hg^{2+} and S species where Hg^{2+} withdraws electrons, placing S atoms in an electron-deficient state, which is consistent with the phenomenon commonly observed in other porous materials.

Conclusions

In summary, the porous luminescent covalent organic imine polymer containing benzothiadiazole (**BTD-MPD-COP**) was successfully synthesized through a hydrothermal method. This material not only demonstrates selective fluorescence detection but also exhibits high efficiency in the removal of Hg^{2+} ions from aqueous solutions. Our research indicates that the incorporation of imine bonds to enhance long-range π-conjugated structures significantly improves the fluorescence performance of the material, while the S–Hg interaction substantially increases its adsorption capacity for Hg^{2+}. Furthermore, **BTD-MPD-COP** displays a high saturation capacity for Hg^{2+} and excellent cycling stability, allowing for repeated use after desorption without significant loss of adsorption capability, which can prove widely applicable for rapid adsorption and removal of Hg^{2+} in aqueous environments. Indeed, this work presents a universal strategy for developing high-performance bifunctional materials by introducing functional groups to modify COPs.

Conflicts of interest

The authors declare no conict of interest.

Data availability

The data supporting this article have been included as part of the supplementary information (SI). Supplementary information: the further experimental details of **BTD** synthesis. See DOI: https://doi.org/10.1039/d5ra09294a.

References

1 T. Dey and F. Dominici, COVID-19, Air Pollution, and Racial Inequity: Connecting the Dots, *Chem. Res. Toxicol.*, 2021, **34**(3), 669–671.

2 Y. Zhang, Y. Sun, L. Cai, Y. Gao and Y. Cai, Optical fiber sensors for measurement of heavy metal ion concentration: A review, *Measurement*, 2020, **158**, 107742.

3 K. H. H. Aziz, F. S. Mustafa, K. M. Omer, S. Hama, R. F. Hamarawf and K. O. Rahman, Heavy metal pollution in the aquatic environment: efficient and low-cost removal approaches to eliminate their toxicity: a review, *RSC Adv.*, 2023, **13**, 17595–17610.

4 L. Liu, M. Hou, Q. Yin and Y. Liu, Toxic heavy metal ions contamination in the aqueous environment, its toxicity and methods of microbial remediation, *Green Chem. Lett. Rev.*, 2024, **17**, 2317824.

5 H. J. Sadiq Hawezy, A. F. Qader, R. A. Omer and L. Abd Ali, Magnetic nanoparticles for efficient heavy metal removal: synthesis, adsorption capacity, and key experimental parameters, *Rev. Inorg. Chem.*, 2025, **45**, 587–596.

6 H. Xi, B. Liu, X. Li, X. Long, Y. Sun, W. Wang and H. Wang, Microbial extracellular electron transfer: A promising strategy for heavy metal removal mechanisms, regulation and future development, *J. Water Process Eng.*, 2025, **71**, 107416.

7 D. Udhayakumari, Review on fluorescent sensors-based environmentally related toxic mercury ion detection, *J. Inclusion Phenom. Macrocyclic Chem.*, 2022, **102**, 451–476.

8 S. Chakraborty, K. Das and S. Halder, A review on chemo sensors and fluro sensors of mercury ions, *Inorg. Chim. Acta*, 2024, **566**, 122026.

9 X. Cheng, T. Luo, F. Chu, B. Feng, S. Zhong, F. Chen, J. Dong and W. Zeng, Simultaneous detection and removal of mercury (II) using multifunctional fluorescent materials, *Sci. Total Environ.*, 2023, **905**, 167070.

10 Z. Yuan, Y. Yang, P. Lv and H. Zhu, Recent Progress in Small-Molecule Fluorescent Probes for Detecting Mercury Ions, *Crit. Rev. Anal. Chem.*, 2020, **52**, 250–274.

11 D. Dai, J. Yang, Y. Wang and Y. Yang, Recent Progress in Functional Materials for Selective Detection and Removal of Mercury(II) Ions, *Adv. Funct. Mater.*, 2020, **31**, 2006168.

12 Y. S. Ridwan, S. Wyantuti, A. A. Sari and Y. W. Hartati, Review—Towards Mercury Free: Ion Imprinted Polymer-Based Electrochemical Sensors for Monitoring of Mercury(II), *J. Electrochem. Soc.*, 2023, **170**, 127503.

13 Q. Chen, Y. Yao, X. Li, J. Lu, J. Zhou and Z. Huang, Comparison of heavy metal removals from aqueous solu-

tions by chemical precipitation and characteristics of precipitates, *J. Water Process Eng.*, 2018, **26**, 289–300.

14 Y. Zhang and X. Duan, Chemical precipitation of heavy metals from wastewater by using the synthetical magnesium hydroxy carbonate, *Water Sci. Technol.*, 2020, **81**, 1130–1136.

15 G. S. Nyamato, Perspectives and prospects of chelation extraction of heavy metals from wastewater: A review, *Water Sci. Technol.*, 2023, **88**, 47–61.

16 P. S. Gahlaut, D. Gautam, K. Yadav and B. Jana, Supramolecular Gels for the Sensing and Extraction of Heavy Metal Ions from Wastewater, *J. Mol. Struct.*, 2022, **1272**, 134152.

17 F. A. Janjhi, D. Janwery, I. Chandio, S. Ullah, F. Rehman, A. A. Memon, J. Hakami, F. Khan, G. Boczkaj and K. H. Thebo, Recent Advances in Graphene Oxide-Based Membranes for Heavy Metal Ions Separation, *ChemBioEng Rev.*, 2022, **9**, 574–590.

18 B. Pospiech and W. Kujawski, Ionic liquids as selective extractants and ion carriers of heavy metal ions from aqueous solutions utilized in extraction and membrane separation, *Rev. Chem. Eng.*, 2015, **31**, 179–191.

19 S. Liu, Y. Cai, M. Du, J. Liu, X. Zhang, H. Yuan, Z. Xu, X. Chen, X. Kan, S. Zhang, L. Zhong and S. Ma, Research on Adsorption of Heavy Metal Ions by Polysaccharide Hydrogels, *ChemistrySelect*, 2024, **9**, e202401752.

20 B. Chen, L. Li, L. Liu and J. Cao, Effective adsorption of heavy metal ions in water by sulfhydryl modified nano titanium dioxide, *Front. Chem.*, 2023, **10**, 1072139.

21 U. Upadhyay, I. Sreedhar, S. A. Singh, C. M. Patel and K. L. Anitha, Recent advances in heavy metal removal by chitosan based adsorbents, *Carbohydr. Polym.*, 2020, **251**, 117000.

22 H. S. Lee and H. S. Shin, Competitive adsorption of heavy metals onto modified biochars: Comparison of biochar properties and modification methods, *J. Environ. Manage.*, 2021, **299**, 113651.

23 D. Udhayakumari, Advancements in nanomolar detection: reviewing colorimetric and fluorescence chemosensors for toxic ion detection, *J. Coord. Chem.*, 2024, **77**, 1402–1436.

24 S. S. Alharthi, A review on indole-based colorimetric and fluorescence sensors for the detection of heavy metal ions, *Chem. Pap.*, 2023, **77**, 7379–7394.

25 B. Balusamy, A. Senthamizhan and T. Uyar, Functionalized Electrospun Nanofibers as a Versatile Platform for Colorimetric Detection of Heavy Metal Ions in Water: A Review, *Materials*, 2020, **13**, 2421.

26 Z. Chen, Z. Zhang, J. Qi, J. You, J. Ma and L. Chen, Colorimetric detection of heavy metal ions with various chromogenic materials: Strategies and applications, *J. Hazard. Mater.*, 2022, **441**, 129889.

27 W. Zhan, Y. Su, X. Chen, H. Xiong, X. Wei, X. Huang and Y. Xiong, Aggregation-Induced Emission Luminogen-Encapsulated Fluorescent Hydrogels Enable Rapid and Sensitive Quantitative Detection of Mercury Ions, *Biosensors*, 2023, **13**, 421.

28 Y. Qiu, J. Yang, J. Zhou and Z. Wu, Sulfhydryl-functionalized anisotropic photonic crystal hydrogels for visual Hg^{2+} detection and adsorption in cinnabar mine water area, *J. Colloid Interface Sci.*, 2025, **694**, 137689.

29 D. Dai, Z. Li, J. Yang, C. Wang, J. Wu, Y. Wang, D. Zhang and Y. Yang, Supramolecular Assembly-Induced Emission Enhancement for Efficient Mercury(II) Detection and Removal, *J. Am. Chem. Soc.*, 2019, **141**, 4756–4763.

30 X. Gao, B. Liu and X. Zhao, Thiol-decorated defective metal-organic framework for effective removal of mercury(II) ion, *Chemosphere*, 2023, **317**, 137891.

31 F. Pan, C. Tong, Z. Wang, F. Xu, X. Wang, B. Weng, D. Pan and R. Zhu, Novel sulfhydryl functionalized covalent organic frameworks for ultra-trace Hg^{2+} removal from aqueous solution, *J. Mater. Sci. Technol.*, 2021, **93**, 89–95.

32 N. Huang, L. Zhai, H. Xu and D. Jiang, Stable Covalent Organic Frameworks for Exceptional Mercury Removal from Aqueous Solutions, *J. Am. Chem. Soc.*, 2017, **139**, 2428–2434.

33 T. Skorjanc, D. Shetty and M. Valant, Covalent Organic Polymers and Frameworks for Fluorescence-Based Sensors, *ACS Sens.*, 2021, **6**, 1461–1481.

34 T. Skorjanc, D. Shetty and A. Trabolsi, Pollutant removal with organic macrocycle-based covalent organic polymers and frameworks, *Chem*, 2021, **7**, 882–918.

35 J. Liu, Y. Chen, X. Jiang, M. Lin, X. Zeng and C. Zhou, Hydrophilic Three-Dimensional Covalent Organic Polymer Membranes for Aqueous Molecular Separation, *ACS Appl. Eng. Mater.*, 2025, **3**, 2663–2671.

36 S. B. Yu, F. Lin, J. Tian, J. Yu, D. W. Zhang and Z. T. Li, Water-soluble and dispersible porous organic polymers: preparation, functions and applications, *Chem. Soc. Rev.*, 2022, **51**, 434–449.

37 P. Puthiaraj, Y. R. Lee, S. Zhang and W. S. Ahn, Triazine-based covalent organic polymers: design, synthesis and applications in heterogeneous catalysis, *J. Mater. Chem. A*, 2016, **4**, 16288–16311.

38 N. Baig, S. Shetty, S. A. Wahed, A. Hassan, N. Das and B. Alameddine, Designing highly porous three-dimensional triazine-bearing covalent organic polymers as prominent adsorbents of carbon dioxide and iodine, *Mater. Today Chem.*, 2024, **41**, 102339.

39 H. Sun, J. Li, W. Liang, X. Gong, A. Jing, W. Yang, H. Liu and S. Ren, Porous Organic Polymers as Active Electrode Materials for Energy Storage Applications, *Small Methods*, 2023, **8**, 2301335.

40 Z. Xiang, D. Cao and L. Dai, Well-defined two dimensional covalent organic polymers: rational design, controlled syntheses, and potential applications, *Polym. Chem.*, 2015, **6**, 1896–1911.

41 S. Y. Ding, M. Dong, Y. W. Wang, Y. T. Chen, H. Z. Wang, C. Y. Su and W. Wang, Thioether-Based Fluorescent Covalent Organic Framework for Selective Detection and Facile Removal of Mercury(II), *J. Am. Chem. Soc.*, 2016, **138**, 3031–3037.

42 M. Thommes, K. Kaneko, A. V. Neimark, J. P. Olivier, F. Rodriguez-Reinoso, J. Rouquerol and K. S. W. Sing,

Physisorption of gases, with special reference to the evaluation of surface area and pore size distribution, *Pure Appl. Chem.*, 2015, **87**, 1051–1069.

43 H. B. Sun, S. J. Liu, T. C. Ma, N. N. Song, Q. Zhao and W. Huang, An excellent BODIPY dye containing a benzo [2,1,3]thiadiazole bridge as a highly selective colorimetric and fluorescent probe for Hg^{2+} with naked-eye detection, *New J. Chem.*, 2011, **35**, 1194–1197.

44 L. Guo, X. Zeng and D. Cao, Porous covalent organic polymers as luminescent probes for highly selective sensing of Fe^{3+} and chloroform: Functional group effects, *Sens. Actuators, B*, 2016, **226**, 273–278.